The Pattern of Retinal Ganglion Cell Loss in Wolfram Syndrome is Distinct From Mitochondrial Optic Neuropathies

PIERO BARBONI, GIULIA AMORE, MARIA LUCIA CASCAVILLA, MARCO BATTISTA, GIULIO FRONTINO, MARTINA ROMAGNOLI, LEONARDO CAPORALI, CRISTINA BALDOLI, LAURA LUDOVICA GRAMEGNA, ELISA SESSAGESIMI, RICCARDO BONFANTI, ANDREA ROMAGNOLI, ROBERTA SCOTTI, MARIA BRAMBATI, MICHELE CARBONELLI, VINCENZO STARACE, CLAUDIO FIORINI, ROBERTA PANEBIANCO, VINCENZO PARISI, CATERINA TONON, FRANCESCO BANDELLO, VALERIO CARELLI, AND CHIARA LA MORGIA

• PURPOSE: To describe the clinical phenotype of a cohort of patients with Wolfram syndrome (WS), focusing on the pattern of optic atrophy correlated with brain magnetic resonance imaging (MRI) measurements, as compared with patients with *OPA1*-related dominant optic atrophy (DOA).

• DESIGN: Retrospective, comparative cohort study.

• METHODS: We reviewed 25 patients with WS and 33 age-matched patients affected by *OPA1*-related DOA. Ophthalmologic, neurologic, endocrinologic, and MRI data from patients with WS were retrospectively retrieved. Ophthalmologic data were compared with data from patients with *OPA1*-related DOA and further analyzed for age dependency dividing patients in age quartiles. In a subgroup of patients with WS, we correlated the structural damage assessed by optical coherence tomography (OCT) with brain MRI morphologic measurements. Visual acuity (VA), visual field mean defect (MD), retinal nerve fiber layer (RNFL), and ganglion cell layer (GCL) thickness were assessed by OCT and MRI morphologic measurements of anterior and posterior visual pathways.

• RESULTS: Optic atrophy was present in 100% of patients with WS. VA, MD, and RNFL thickness loss were worse in patients with WS with a faster decline since early age as compared with patients with DOA, who displayed a more stable visual function over the years. Conversely, GCL sectors were overall thinner in patients with DOA since early age compared to patients with WS, in which GCL thickness started to decline later in life. The neuroradiologic subanalysis on 11 patients with WS exhibited bilateral thinning of the anterior optic pathway, especially the prechiasmatic optic nerves and optic tracts. Optic tract thinning was significantly correlated with GCL thickness but not with RNFL parameters.

• CONCLUSIONS: Our results showed a generally more severe and diffuse degeneration of both anterior and posterior visual pathways in patients with WS, with fast deterioration of visual function and structural OCT parameters since early age. The pattern observed with OCT suggests that retinal ganglion cell axonal degeneration (ie, RNFL) precedes cellular body atrophy (ie, GCL) by about a decade. This differs substantially from DOA, in which a more stable visual function is evident with predominant early loss of GCL, indirectly supporting the lack of a primary mitochondrial dysfunction in patients with WS. (Am J Ophthalmol 2022;241: 206–216. © 2022 Elsevier Inc. All rights reserved.)

AJO.com Supplemental Material available at AJO.com.

Accepted for publication March 16, 2022.

From the Department of Ophthalmology (P.B., M.L.C., M.Ba., M.Br., V.S., F.B.), University Vita-Salute, IRCCS Ospedale San Raffaele, Milan, Italy; Studio Oculistico d'Azeglio (P.B.), Bologna, Italy; Dipartimento di Scienze Biomediche e Neuromotorie (G.A., L.L.G., E.S., M.C., C.T., V.C.), Università di Bologna, Bologna, Italy; Department of Pediatrics (G.F., R.B., A.R.), IRCCS San Raffaele Hospital, Milan, Italy; Diabetes Research Institute (G.F., R.B., A.R.), IRCCS San Raffaele Hospital, Milan, Italy; IRCCS Istituto delle Scienze Neurologiche di Bologna (M.R., L.C., C.F., V.C., C.L.M.), Programma di Neurogenetica, Bologna, Italy; Neuroradiology Unit (C.B., R.S.), IRCCS San Raffaele Scientific Institute, Milan, Italy; IRCCS Istituto delle Scienze Neurologiche di Bologna (L.L.G., E.S., C.T.), Functional and Molecular Neuroimaging Unit, Bologna, Italy; Department of Ophthalmology (R.P.), University of Catania, Catania, Italy; G.B. Bietti Foundation IRCCS (V.P.), Rome, Italy; IRCCS Istituto delle Scienze Neurologiche di Bologna (C.L.M.), UOC Clinica Neurologica, Bologna, Italy

Inquiries to Piero Barboni, Department of Ophthalmology, University Vita-Salute, IRCCS Ospedale San Raffaele, Via Olgettina, Milan, Italy.; e-mail: p.barboni@studiodazeglio.it

Wolfram syndrome (WS, OMIM 222300) is a rare autosomal recessive neurodegenerative disease that in the majority of cases is associated with bi-allelic *WFS1* mutations.[1,2] WS is characterized by childhood-onset diabetes mellitus (DM), optic atrophy (OA), diabetes insipidus (DI), and deafness (D), which represent the cardinal clinical features of the disease (the previous acronym was DIDMOAD).[3] Other common clinical manifestations of the disease may include urinary tract dysfunction (UD) and neurologic and psychiatric disorders, which eventually lead to premature death.[4]

0002-9394/$36.00
https://doi.org/10.1016/j.ajo.2022.03.019

WFS1 encodes for the endoplasmic reticulum (ER) membrane protein Wolframin that has a role in the regulation of cellular and ER $Ca2^+$ homeostasis, Na/K ATPase function, and regulation of the ER stress response.[5] Wolframin is now confirmed to be enriched in the mitochondrial-associated membranes,[6] areas of close juxtaposition between the ER and mitochondria regulating numerous key interorganelle exchanges, in particular $Ca2^+$ flux,[7] which is affected by *WFS1* mutations.[8,9] The mechanism and functional relevance to neurodegeneration of the mitochondrial involvement in WS remains largely unsolved,[10] despite the longstanding debate and series of controversial reports on this issue.[8,9,11–13]

DM and OA are diagnosed within the first decade of life and represent the 2 major criteria for a diagnosis of WS. DM is caused by pancreatic β-cell degeneration leading to a reduction of insulin levels, and it is usually the first manifestation of the disease, even if patients with WS with OA but without DM are also reported.[14] In fact, the genetic and clinical landscape of WS recently expanded, as recessive and dominant forms with virtually identical clinical features may occur, and next-generation sequencing increasingly uncovers recessive forms of isolated OA.[14]

A complex neurologic involvement is also frequent in WS, recently estimated as the third most frequent manifestation after DM and OA, with an early mean age at onset of 15 years.[15] A comprehensive case series described a combination of hypo/anosmia, ataxia, seizures, dysarthria, dysphagia, neurogenic bladder, central apnea, neurogenic upper airway collapse, as well as psychiatric disturbances.[4] Moreover, magnetic resonance imaging (MRI) scans of the brains of patients with WS typically reveals thinning of the optic nerves, optic chiasm, and tracts, but also atrophy of the cerebral and cerebellar cortex, as well as of the hypothalamic region, with prominent brainstem atrophy in particular of the pons, present in a majority of cases.[9,16–18] However, neurologic symptoms are often underestimated and are characterized by a progressive course, with unclear correlation with MRI findings.[12,19,20]

Pathophysiologically, Wolframin has been implicated in brain development and neurodegeneration, also impacting myelination as primary neuropathologic features.[17,21]

OA with or without DM is an early defining manifestation of the disease required for diagnosis. Optical coherence tomography (OCT) studies demonstrated retinal nerve fiber layer (RNFL) thinning in patients without visual loss.[9,14,22–25] Wolframin is expressed in retinal ganglion cells (RGCs) and in the unmyelinated intraretinal RGC axons.[26,27] The degeneration of RGCs leading to axonal loss has been postulated as a pathogenetic mechanism for OA in WS, as widespread axonal pathology is documented in the central nervous system[28,29] including the retinal and optic nerve RGC axons.[30] However, only a few studies evaluated longitudinal changes of OA in WS, as well as the correlation of OA with brain MRI findings.[9,17,25] Overall, the characteristics of OA in WS, how this develops, and the similarities or differences with classical mitochondrial optic atrophies like dominant optic atrophy (DOA) are currently poorly explored. DOA, a relatively more common form of inherited optic neuropathy, is a paradigm for a pathogenic mechanism leading to axonal degeneration consequent to mitochondrial dysfunction, which for the frequent *OPA1* mutation is centered on dysfunctional mitochondrial fusion and dynamics.[10]

We analyzed RGC neurodegeneration in a cohort of patients with WS compared with a well-established mitochondrial optic neuropathy, ie, DOA,[10] proposing the possible course and pattern of RGC/axonal degeneration in both disorders. We also correlated RGC structural damage, as assessed by OCT, with brain MRI features in a subgroup of patients with WS. Finally, we evaluated the correlation, if any, between the WS phenotype and the *WFS1* genotype.

METHODS

• **STUDY POPULATION:** The clinical and genetic data of 25 patients carrying recessive biallelic *WFS1* pathogenic variants were retrospectively analyzed and ophthalmologic, neurologic, endocrinologic, and MRI data were included. The ophthalmologic data of a second cohort, representative of a classical mitochondrial optic neuropathy, including 33 age- and sex-matched patients affected by *OPA1*-related DOA (from here forward DOA), were compared with patients with WS. Patients with WS and DOA were evaluated at the San Raffaele Scientific Institute, Milan, Italy, and the IRCCS Istituto delle Scienze Neurologiche di Bologna, Bologna, Italy. The study adheres to the tenets of the Declaration of Helsinki and was approved by the San Raffaele Hospital, Milan (143/INT/2020) and Bellaria Hospital, Bologna (121/2019/OSS/AUSLBO - 1901), Ethics Committee. Informed consent was obtained from all participants.

• **CLINICAL ASSESSMENTS:** Ophthalmologic, neurologic, and endocrinologic data were collected in patients with WS. Ophthalmologic data included best-corrected visual acuity (VA) using a Snellen chart, color vision tests (Ishihara test), slit-lamp biomicroscopy, Goldman applanation tonometry, color fundus photography, optical coherence tomography (OCT; DRI Triton, Topcon), automated visual field test (Humphrey Field Analyzer, protocol Sita Standard 30-2; Zeiss). OCT protocols included the evaluation of peripapillary RNFL thickness and ganglion cell layer (GCL) segmentation analysis of the macula (GCL is defined as the thickness from the inner boundary of the GCL to the outer boundary of the inner plexiform layer) (Supplementary Material, Figure S1). Only high-quality scans, defined as scans with signal strength $\geq$7, without RNFL discontinuity or misalignment, involuntary saccadic or blinking artifacts, and absence of algorithm segmentation fail-

ure on careful visual inspection, were used for analysis. The images were obtained using a 3-dimensional wide scan protocol with a size of 12 × 9 mm consisting of 256 B-scans, each comprising 512 A-scans. This allowed obtaining images of the macular and optic nerve head region in a single scan. Peripapillary RNFL thickness were measured using a 360° 3.4-mm–diameter circle scan with thicknesses measured across the superior, nasal, inferior, and temporal sectors and segmentation analysis of the macula measured across 6 sectors of the 6-mm–diameter circular annulus centered on the fovea included GCL.

Neurologic symptoms and signs were retrospectively retrieved from the clinical charts. In particular, the presence of cerebellar (including ataxia, dysarthria, nystagmus, and tremor), bulbar or pyramidal involvement, along with signs of polyneuropathy, myoclonus, and neurologic bladder were assessed and their frequency reported. Endocrinologic assessment was also performed to assess the occurrence of DM and DI.

• **NEUROIMAGING:**

MRI evaluation

Two experienced neuroradiologists (L.L.G., C.B.) retrospectively reviewed the available brain MRI scans of 11 patients with WS seen at both study centers. Patients were considered for the analysis if the MRI protocol included a volumetric T1-weighted image (1-mm^3 isotropic voxel) and an axial T2 fluid-attenuated inversion recovery image. The MRI inspection analysis included morphometric and conventional evaluations.

Morphometric MRI evaluation of the anterior optic pathway

Assessments of the optic nerve and optic tract diameters were manually tracked based on the axial T1-weighted reformatted image obtained parallel to the optic nerves and tracts through the optic chiasm as previously reported[31,32] (Supplementary Material, Figure S2).

Conventional brain MRI evaluation of the optic radiation

Axial T2 fluid-attenuated inversion recovery images were visually inspected to evaluate the presence of white matter signal abnormalities (namely increased signal intensity) in the bilateral peritrigonal areas at the level of optic radiation and, if present, it was graded as slight or severe.

MRI morphometric measurements of patients with WS were compared with mean values of a population of adult healthy control subjects selected from the database of the Neuroimaging Laboratory (IRCCS Istituto delle Scienze Neurologiche di Bologna), designed to collect normative values of quantitative magnetic resonance parameters for clinical and research purposes and to normal values reported in the literature for normal control subjects 12 to 18 years of age.[33]

• **GENETIC ANALYSIS:** Genetic analysis was performed by direct sequencing of *WFS1* or by a next-generation sequencing–based diagnostic panel designed for hereditary optic neuropathies, including *WFS1*.[34] Table 1 shows the genetic findings of patients with WS. *OPA1* mutations were also confirmed in all patients with DOA (Supplementary Material, Table S1). To assess a possible genotype/phenotype correlation, different genotypic classes were defined based on the mutation type and their predicted effect on *WFS1* expression, as described by de Heredia and associates[3]: class A, no WFS1 protein produced because of WFS1 mRNA degradation (A1) or because of mRNA and protein degradation (A2) or because of WFS1 protein degradation (A3); class B, reduced expression of a defective WFS1 protein; or class C, expression of a defective WFS1 protein.

• **STATISTICAL ANALYSIS:** The following visual parameters were analyzed: visual acuity (VA), mean defect (MD) at visual field, Ishihara color vision testing, RNFL (average, temporal, superior, nasal, and inferior quadrants), and GCL thickness (average and 6 individual macular sectors: superotemporal, superior, superonasal, inferonasal, inferior, and inferotemporal). The 2 groups (patients with *OPA1*-related optic neuropathy vs patients with *WFS1*-related optic atrophy) were analyzed to compare gender distribution frequency, age, and visual function outcomes.

Patient data (age and gender) were compared using Chi-square and *t* tests, and normality of all continuous variables was checked by using Shapiro-Wilk and Kolmogorov-Smirnov tests. Continuous variables are presented as mean ± standard deviation (or standard error), while categorical variables as absolute and relative frequencies.

Visual outcome variables were compared by means of a linear mixed-effects model (LMM) with the visual outcome as the dependent variable, the group as an independent variable, under a compound symmetry covariance structure and with a patient random effect, while adjusting for age and gender. The random effect was used to take into account the correlation between 2 eyes of the same patient. For visual outcomes with skewed distribution, we applied the clustered Wilcoxon rank sum test using the Rosner-Glynn-Lee method.

Moreover, the *P* value for interaction age × group was computed from the log-likelihood ratio test comparing LMM models with and without the interaction term, and stratified β coefficients (95% confidence interval [CI]) for variables that were effect modifiers (*P* for interaction < .20) are shown. We also evaluated the ophthalmologic parameters in age quartiles (q1 = 11-16 years; q2 = 17-25 years; q3 = 26-40 years; and q4 = 41-58 years).

For the patient with WS subgroup that had both MRI and OCT examinations, Spearman correlation coefficients were used to measure the degree of association between OCT findings and MRI parameters.

TABLE 1. Genetic Features of Patients With Wolfram Syndrome

Patient	Mutation		Mutation Type 1	Mutation		Mutation Type 2	Classification	Inheritance
	DNA 1	Protein 1		DNA 2	Protein 2			
1	c.605A>G	p.Glu202Gly	II	C.1289C>T	p.Ser430Leu	II	A3	Recessive
2	c.409_424du pGGCCGTCG CGAGGCTG	p.Val142Glyfs Ter110	I	c.1628T>G	p.Leu543Arg	II	A2	Recessive
3	c.2104G>A	p.Gly702Ser	II	c.1369A>G	p.Arg457Gly	II	A3	Recessive
4	c.387G>A	p.Trp129Ter)	I	c.1675G>C	p.Ala559Pro	II	A2	Recessive
5	c.2213C>A	p.Ala738Asp	II	c.2213C>A	p.Ala738Asp	II	A3	Recessive
6	c.2452C>T	p.Arg818Cys	II	c.1515_1529del15	p.Val509_Tyr513del	II	A3	Recessive
7	c.2107C>T	p.Arg703Cys	II	c.2107C>T	p.Arg703Cys	II	A3	Recessive
8	c.316-1G>A	Splice defect	I	c.757A>T	p.Lys253Ter	I	A1	Recessive
9	c.409_424du pGGCCGTCGC GAGGCTG	p.Val142Glyfs Ter110	I	c.1381A>C	p.Thr461Pro	II	A2	Recessive
10	c.605A>G	p.Glu202Gly	II	c.1628T>G	p.Leu543Arg	II	A3	Recessive
11	c.2106_2113de lCCGCTTCA	p.Arg703Valfs Ter6	III	c.2106_2113 delCCGCTTCA	p.Arg703ValfsTer6	III	C	Recessive
12	c.1553T>A	p.Met518Lys	II	c.1553T>A	p.Met518Lys	II	A3	Recessive
13	c.409_424du pGGCCGTCGC GAGGCTG	p.Val142Glyfs Ter110	I	c.2104G>A	p.Gly702Ser	II	A2	Recessive
14	c.977C>T	p.Ala326Val	II	c.977C>T	p.Ala326Val	II	A3	Recessive
15	c.1928T>G	p.Ile643Ser	II	c.2194C>T	p.Arg732Cys	II	A3	Recessive
16	c.1928T>G	p.Ile643Ser	II	c.2194C>T	p.Arg732Cys	II	A3	Recessive
17	c.2002C>T	p.Gln668Ter	III	c.2126T>G	p.Val709Gly	II	B	Recessive
18	c.1628T>G	p.Leu543Arg	II	c.2104G>A	p.Gly702Ser	II	A3	Recessive
19	c.370T>C	p.Cys124Arg	II	c.2213C>A	p.Ala738Asp	II	A3	Recessive
20	c.1675 G>A	p.Ala559Thr	II	c.1381A>C	p.Thr461Pro	II	A3	Recessive
21	c.605A>G	p.Glu202Gly	II	c.605A>G	p.Glu202Gly	II	A3	Recessive
22	c.1541T>G	p.Leu514Arg	II	c.1541T>G	p.Leu514Arg	II	A3	Recessive
23	c.387G>A	p.Trp129Ter	I	c.387G>A	p.Trp129Ter	I	A1	Recessive
24	c.1381A>C	p.Thr461Pro	II	c.2099G>A	p.Trp700Ter	III	B	Recessive
25	c.2206G>A	p.Gly736Ser	II	c.2206G>A	p.Gly736Ser	II	A3	Recessive

WFS1 mutation details are provided as DNA and protein changes with corresponding mutation type and classification.

Two-sided *P* values are presented. Statistical analyses were carried out with R (version 4.0.0) and IBM SPSS Statistics for Windows (version 20.0; IBM Corp) software.

RESULTS

The demographic data of subjects analyzed are reported in Table 2. The mean age of patients with WS was 29.5 ± 12.7 years (range 11-58 years). The main clinical features of the 25 patients with WS are reported in Table 3; DM was the first clinical feature of the disease at onset and present in 80% of patients, whereas the most frequent feature was OA (100%). DI was present in 20% of cases. Neurologic symptoms were documented in 60% of cases, cerebellar signs being the most common. The relative frequency of each neurologic sign is reported Supplementary Material Table S2.

• **OPHTHALMOLOGIC EVALUATION:** The visual function parameters, including VA, MD, and color vision, were all significantly more severe in patients with WS compared with patients with patients with DOA (Table 4).

The average and sectorial RNFL thicknesses were significantly lower in patients with WS compared with patients with DOA even though this difference was less evident for the temporal quadrant (Table 4). Conversely, the GCL analysis showed a significant thinning only of the inferonasal sector in patients with DOA. All other sectors were thinner in patients with DOA without reaching significance except for the superior and superotemporal sectors,

TABLE 2. Demographic Data

	WS	DOA	*P* Value
Subjects, n (%)	25 (43.1)	33 (56.9)	
Gender, n (%)			.3
Female	15 (60)	14 (42.4)	
Male	10 (40)	19 (57.6)	
Age (y), mean ± SD	29.5 ± 12.7	27 ± 14.2	.5

DOA = dominant optic atrophy; SD = standard deviation; WS = Wolfram syndrome.

Chi-square test was performed with gender variable and *t* test was performed with age variable.

which were thicker in patients with DOA compared with patients with WS (Table 4).

We also looked at VA changes in relation to the age at clinical assessment in the WS and DOA groups. Patients with WS and patients with DOA started with a similar VA loss. However, across the first and the second quartiles, the progression of VA decrease was faster in patients with WS compared with patients with DOA, which remained largely stable over the decades (Figure 1). Differently, the MD reduction was more severe in patients with WS compared with patients with DOA since the first quartile but with a clear progression over time as for VA. MD remained, instead, substantially stable in DOA over the decades (Figure 1).

We also evaluated the interaction between groups (WS and DOA) and age using the likelihood-ratio test (Supplementary Material, Tables S3 and S4). The likelihood-ratio test showed the existence of a significant group × age interaction for nasal RNFL ($P = .16$) and for superior-temporal GCL ($P = .15$) thickness with a significant association between OCT parameters and age only in patients with WS (Figure 2).

RNFL thinning was more evident in WS compared with DOA since the first quartile of life (Figure 2). Moreover, progressive RNFL thinning with age in patients with WS was evident in all quadrants and in particular in the nasal quadrant, which was statistically significant (likelihood ratio = 0.16; Supplementary Materials Tables S3 and S4). In contrast, a trend in progression of RNFL thinning in patients with DOA was observed, particularly in the superior sector.

In distinction with RNFL, the GCL was thicker in patients with WS compared with patients with DOA in the first quartiles and became thinner after the second quartile, whereas the GCL thinning was more evident in patients with DOA than in patients with WS in the second quartile, remaining substantially stable over time (Figure 3). The nasal sector appeared more affected as compared with the other sectors in patients with DOA. The superior temporal sector showed the most and significant thinning (likelihood ratio = 0.15) over time in patients with WS compared with patients with DOA, for which it was substantially stable over time (Supplementary Table 3 and 4).

• **NEURORADIOLOGIC FINDINGS:** Brain MRI findings are reported in the Supplementary Material (Table S5). All patients with WS (N = 11) exhibited bilateral thinning of the anterior optic pathway and, in particular, in patients >18 years of age (n = 5; mean 31 years, range 22-47 years), the mean diameter of the prechiasmatic optic nerves was 3.0 ± 0.4 mm and the mean diameter of the optic tracts was 2.2 ± 0.3 mm. In patients <18 years of age (n = 6; mean 14 years, range 12-17 years) the mean diameter of the prechiasmatic optic nerves was 3.3 ± 0.3 mm, and the mean diameter of the optic tracts was 2.4 ± 0.5 mm.

All measures were smaller than mean values for normal control subjects 22 to 51 years of age (prechiasmatic optic nerve: 4.0 ± 0.4 mm; optic tract: 3.6 ± 0.4 mm) and for normal control subjects 12 to 18 years of age (prechiasmatic optic nerve: 3.5 ± 0.3 mm; optic tract: 2.9 ± 0.3 mm).[33] At visual inspection, increased signal intensity in the bilateral peritrigonal areas was observed in 10 of 11 patients (90.9%) in T2-weighted images, with a slight increase in 8 patients and a severe increase in 2 patients. Optic tract thinning was significantly correlated with GCL average thickness ($P < .0004$) and with all GCL sectors, in particular with the superior sectors (Supplementary Material Table S5) but not with RNFL parameters. Prechiasmatic optic nerves as measured by brain MRI were not significantly correlated with RNFL and GCL parameters.

TABLE 3. Clinical Features of Patients With Wolfram Syndrome

	Patients (n)	Rate of Patients (%), n = 25	Reported Mean Age at Onset (y), Mean ± SD
Diabetes mellitus	20	80	10.8 ± 5.8
Optic atrophy	25	100	15.5 ± 8.8
Urologic defect	14	56	26.4 ± 12.6
Hearing defect	8	32	25.3 ± 18.3
Diabetes insipidus	5	20	15.0 ± 7.0
Neurologic symptoms	15	60	Not available

SD = standard deviation.

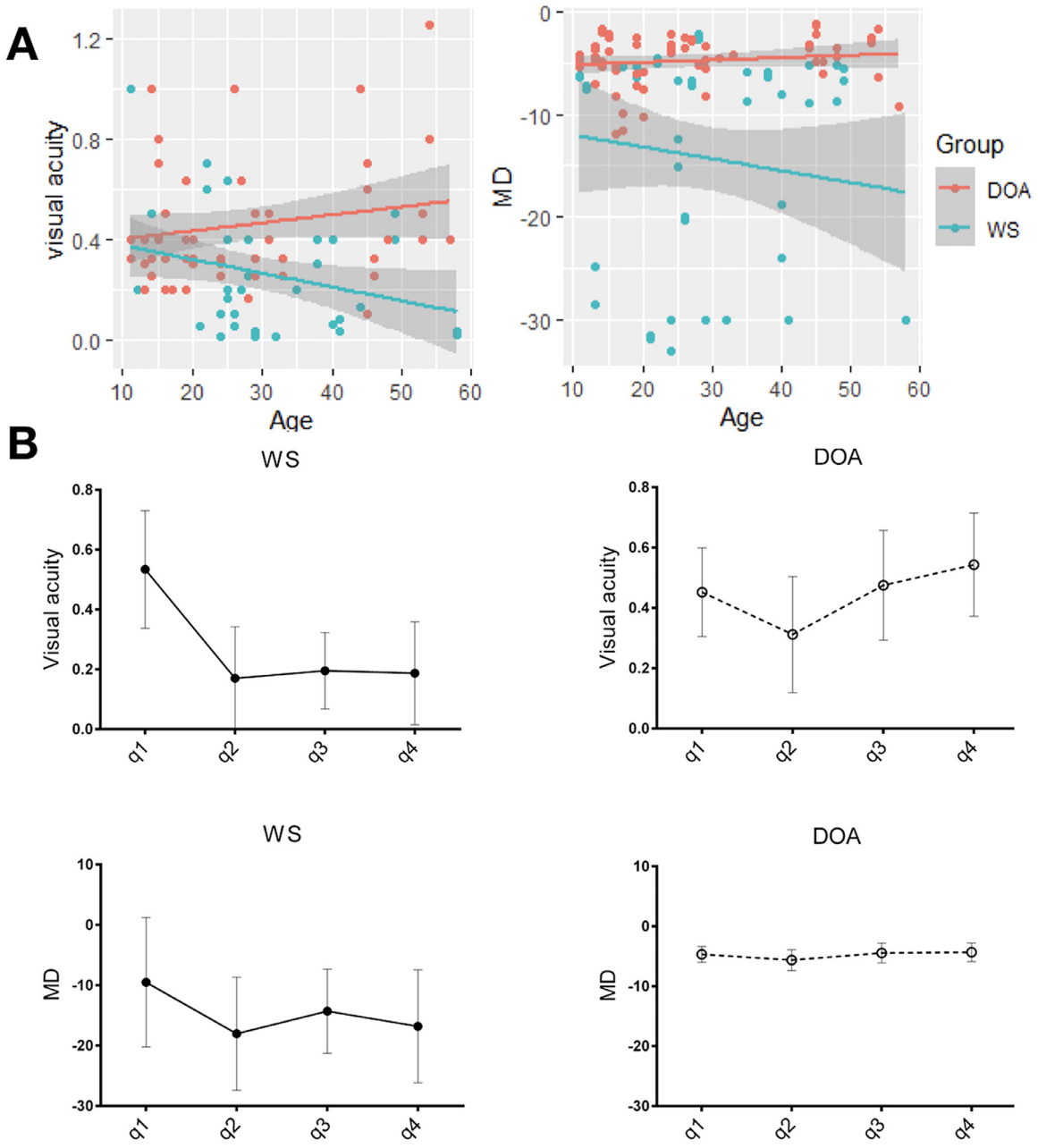

FIGURE 1. A. Scatterplots showing visual acuity by the Snellen chart (left) and mean deviation (MD) by visual field testing (right) against age (on the x axis) with the group regression line and confidence intervals shaded in gray. B. Top panels show figure shows plots of estimated marginal means of visual acuity by the Snellen chart from LMM in patients with WS (left) and patients with DOA (right) for each age quartile (q1 = 11-16 years of age; q2 = 17-25 years of age; q3 = 26-40 years of age; and q4 = 41-58 years of age). Bottom panels show plots of estimated marginal means of MD by visual field testing from LMM in patients with WS (left) and patients with DOA (right). Error bars represent the standard error. DOA = dominant optic atrophy; LMM = linear mixed regression model; WS = Wolfram syndrome.

• GENETIC AND CLINICAL FINDINGS: Grouping the patients by genetic classification, most of the patients (n = 16) belonged to class A3 (64%) and for this reason no statistical analysis was considered meaningful (Supplementary Material Table S6). The patients belonging to class A1 had better visual function and structural preservation and class C the worst, but the low sample size did not allow us to reach any conclusions.

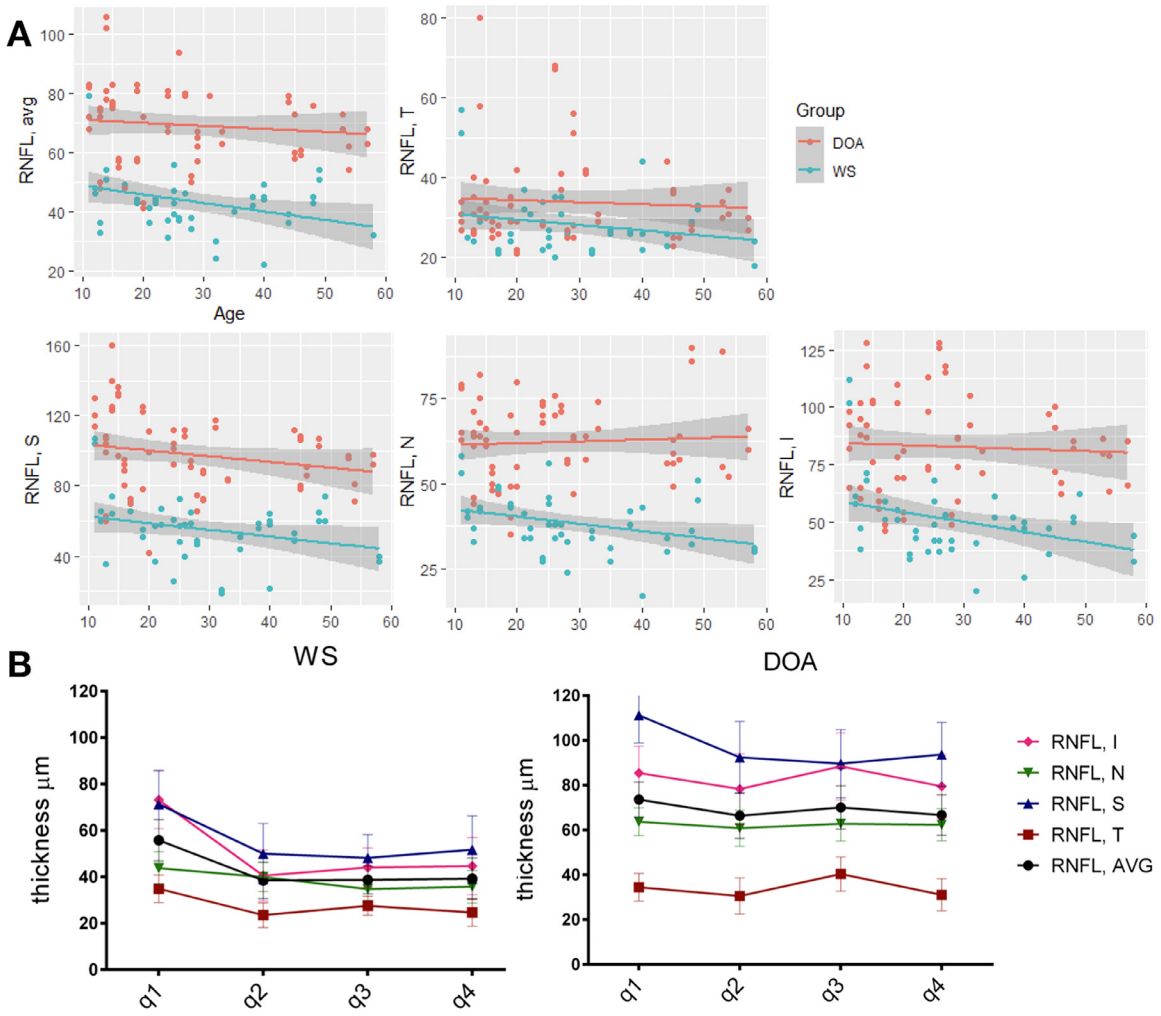

FIGURE 2. A. Scatterplots displaying RNFL thickness (µm) quadrants (average [avg], temporal [T], superior [S], nasal [N], and inferior [I]) against age (x axis) with the group regression line and confidence intervals shaded in gray. B. Plots of estimated marginal means of RNFL thickness quadrants from LMM in patients with WS (left) and patients with DOA (right) for each age quartile (q1 = 11-16 years of age; q2 = 17-25 years of age; q3 = 26-40 years of age; and q4 = 41-58 years of age). Error bars represent the standard error. DOA = dominant optic atrophy; LMM = linear mixed regression model; RNFL = retinal nerve fiber layer; WS = Wolfram syndrome.

DISCUSSION

In the current study we reported the clinical and genetic findings of a cohort of patients with WS compared with a classical mitochondrial optic neuropathy such as DOA, which may point to a 2-step neurodegenerative process in WS. In fact, by considering the pattern of OCT findings over decades, the timing of RGC axonal degeneration precedes RGC cellular body atrophy by about a decade. This introduces a substantial difference with DOA, highlighting a generally more severe and diffuse pathology in WS than in DOA, which progresses over time. DOA has been suggested to be a congenital or early loss of RGCs, with little progression and prolonged stability over decades,[35] as confirmed by the current data. Overall, these results revealed a different timing and pattern of RGC/axonal degeneration in WS compared with DOA.

Optic atrophy represents the major defining clinical hallmark of WS, either with recessive or dominant transmission, occurring at an early age and presenting occasionally also without the characteristic association with DM.[14] In fact, in our series, OA was present in 100% of cases, whereas DM was observed in 80% of cases. The RGC damage has been already reported in WS by previous OCT studies.[9,23,30] However, we considered our results in relation to the patient's age, showing an early and fast deterioration of functional and structural parameters in WS that was more evident between the first and second quartiles, different from what is seen in patients with DOA. In fact, in WS

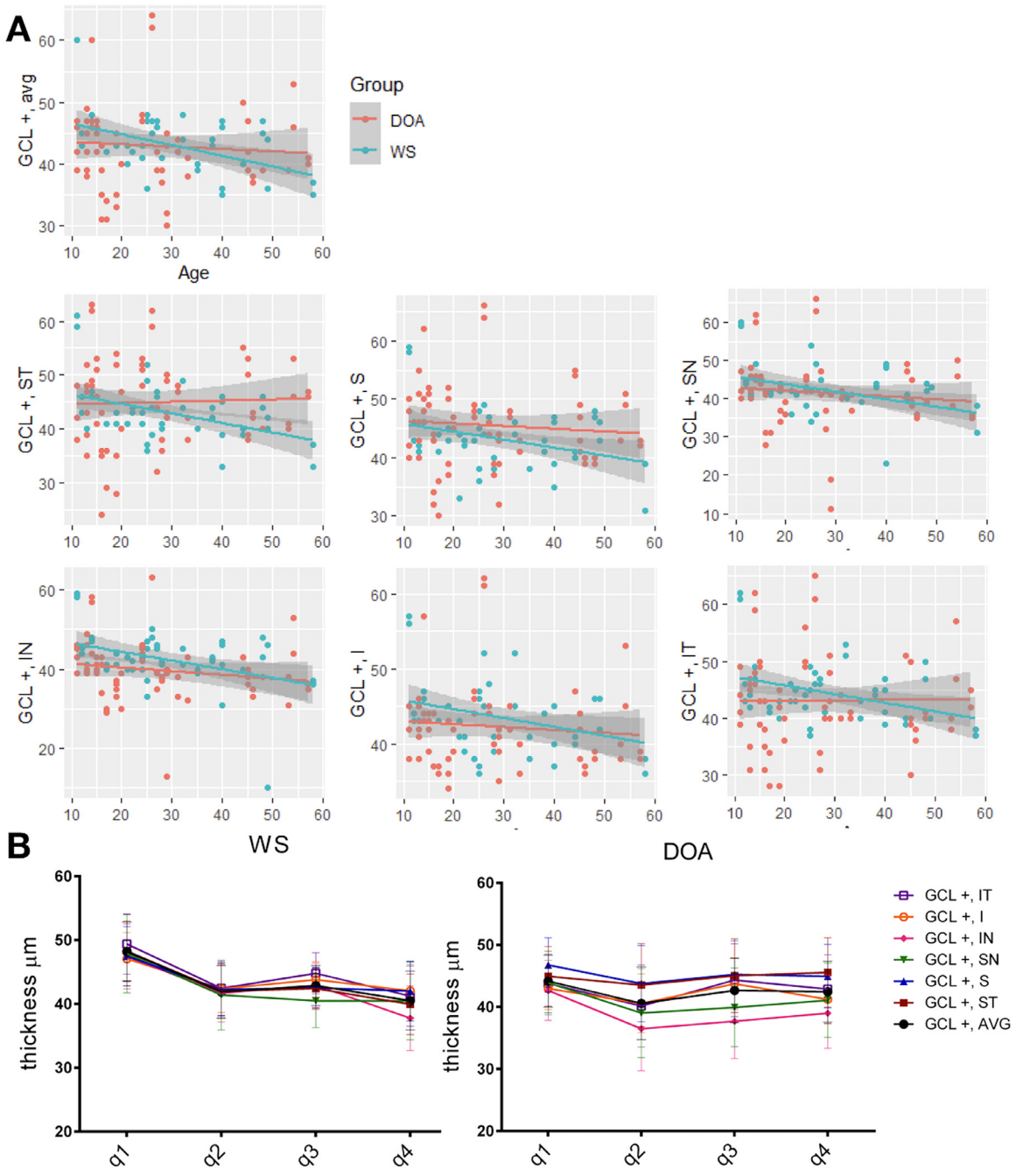

FIGURE 3. A. Scatterplots showing GCL thickness (µm) sectors (average [avg], superotemporal [ST], superior [S], superonasal [SN], inferonasal [IN], inferior [I], and inferotemporal [IT]) against age (x axis) with the group regression line and confidence intervals shaded in grey. B. Plots of estimated marginal means of GCL thickness (µm) sectors from LMM in patients with WS (left) and patients with DOA (right) for each age quartile (q1 = 11-16 years of age; q2 = 17-25 years of age; q3 = 26-40 years of age; and q4 = 41-58 years of age). Error bars represent the standard error. DOA = dominant optic atrophy; GCL = ganglion cell layer; LMM = linear mixed regression model; WS = Wolfram syndrome.

we observed earlier damage of visual fields and RNFL thinning associated with a relative preservation of GCL in the first quartile of life. In comparison, patients with DOA had thicker RNFL in all quadrants, whereas GCL was overall thinner at at early age compared with patients with WS.

These data suggest that WS damage does not follow the typical pattern of a mitochondrial optic neuropathy, characterized by a preferential loss of fibers in the papillomacular bundle, in line with previous studies demonstrating that a primary mitochondrial dysfunction is lacking in

TABLE 4. Ophthalmologic Parameters

	WS	DOA	*P* Value
Eyes, n	50	66	
Right eyes	25	33	
Left eyes	25	33	
VA, decimal scale	0.26 ± 0.05	0.46 ± 0.04	.01[a]
MD, dB	−14.6 ± 1.4	−4.6 ± 1.2	<.001[a]
Eyes, n	50	56	
Right eyes	25	28	
Left eyes	25	28	
Ishihara's test	0	7	<.001[a]
Eyes, n	46	66	
Right eyes	23	33	
Left eyes	23	33	
RNFL AVG (μm)	42.4 ± 2.4	69.5 ± 2.0	<.001[a]
RNFL T (μm)	27.7 ± 1.9	34.1 ± 1.6	.01[a]
RNFL S (μm)	54.3 ± 4	98.1 ± 3.3	<.001[b]
RNFL N (μm)	37.7 ± 1.9	62.4 ± 1.6	<.001[b]
RNFL I (μm)	49.6 ± 3.8	83.0 ± 3.1	<.001[a]
Eyes, n	46	64	
Right eyes	23	32	
Left eyes	23	32	
GCL AVG (μm)	43.3 ± 1.3	42.7 ± 1.1	.65[a]
GCL ST (μm)	43.1 ± 1.4	44.8 ± 1.2	.22[a]
GCL S (μm)	43.4 ± 1.3	45.4 ± 1.1	.25[b]
GCL SN (μm)	42.2 ± 1.6	41.3 ± 1.3	.67[a]
GCL IN (μm)	42.7 ± 1.5	39.4 ± 1.2	.02[a]
GCL I (μm)	43.7 ± 1.1	42.2 ± 0.9	.20[a]
GCL IT (μm)	44.5 ± 1.4	43 ± 1.2	.42[b]

AVG = average; DOA = dominant optic atrophy; GCL = ganglion cell layer; I = inferior; IN = inferonasal; IT = inferotemporal; MD = mean defect; N = nasal; RNFL = retinal nerve fiber layer; S = superior; SN = superonasal; ST = superotemporal; T = temporal; VA = visual acuity; WS = Wolfram syndrome.

[a]Comparison of optical coherence tomography variables normally distributed between WS and DOA using the clustered Wilcoxon rank sum test and the Rosner-Glynn-Lee method.

[b]Comparison of optical coherence tomography variables normally distributed between WS and DOA using multivariate linear mixed regression models (linear mixed-effects model, maximum likelihood method, random intercept, or compound symmetry). *P* value referred to "group" predictor of multivariate linear mixed-effects model adjusted for gender and age.

WS.[9] Moreover, we found in WS the presence of a progressive worsening of functional (VA and MD) and structural (RNFL and GCL) parameters, in contradistinction with a substantial stability pattern in DOA.

This is the first OCT study reporting the comparison between WS and DOA with the inclusion of correlative analysis of RNFL with GCL sectors in relation to age, which highlights the possibility that axonal damage may precede the involvement of RGC cell body. Moreover, the RNFL thinning corresponds to an early and severe visual function loss in WS followed by a progressive damage of the GCL. Overall, these findings have relevant implications also for visual prognosis in WS.

The exact mechanism leading to early damage of the axons in WS is presently unknown. Wolframin is highly expressed in the brain and optic nerve and has a relevant role in brain development and particularly for axonal myelination.[17,21] Moreover, neuronal dysfunction has been reported in a fly homolog of *WFS1*.[36] The critical point is how and when active neurodegeneration becomes superimposed on the defective development. Neurodegeneration is well documented to occur by the progressive nature of CNS deterioration, and our current findings may indicate a retrograde axonal degeneration, for which developmental hypomyelination may play a role.[37]

We also looked at the neuroradiologic findings of WS, focusing on the brain MRI signature of visual system degeneration showing anterior visual pathway atrophy and increased signal intensity in the bilateral peritrigonal areas corresponding to optic radiations. We correlated brain MRI morphometric evaluation to OCT measurements showing a significant correlation only between the GCL and the optic tract thinning, supporting the concept that the retinal cell body degeneration best correlates with the anterior optic pathway atrophy commonly observed in these patients. Instead, the lack of correlation of MRI measurements with RNFL thinning can be explained by the severe RNFL atrophy (floor effect) already present at the time of MRI scans. Another consideration is that OCT measurements do not include the myelin component, as myelination starts posterior to the lamina cribrosa, conversely with MRI that captures the myelin signal along the optic nerves and tracts. Moreover, we cannot exclude that the small sample size, the different disease duration at examinations, and the resolution of the 2 techniques may impact the correlative results. One other study investigated the possible correlations between OCT and visual pathway measurements at MRI, not including optic radiations and comparing WS to patients with DM. A significant correlation was found only between the superior quadrant of peripapillary RNFL and the intraorbital part of the optic nerve, a finding that remains difficult to interpret.[25]

Our study also focused on the presence of white matter signal abnormalities in areas corresponding to the optic radiations. Previous histopathologic studies reported patchy demyelination and axonal degeneration of the same areas, as well as altered signal of occipital white matter, which was observed in 1 single case report at MRI evaluation.[17,38]

DM was evident in 80% of the patients with WS, highlighting that the presence of DM is not a mandatory feature of the disease and clears the argument made in the literature that optic atrophy is a secondary feature of diabetes. This somehow shifts the diagnostic paradigm and clears the argument on optic atrophy as a secondary feature of diabetes

that recurred in literature[9] and emphasizes the importance to screen also for *WFS1* mutation in the presence of childhood onset optic atrophy even in the absence of DM, no matter which Mendelian transmission may occur. Neurologic symptoms were quite common in our cohort (60%) in line with previous reports.[1] DI showed an earlier age at onset in our series compared with other described case series.[39]

Concerning the genotype–phenotype correlation, because most patients were in class A3 a statistical analysis was not possible and larger cohort studies are needed.

Limitations of the current study are the relatively small sample size of our cohort due to the rarity of the disease and the retrospective nature of the analysis. Furthermore, this is a cross-sectional study with single time points for each patient, thus our analyses using the timeline distribution of the results only raises a hypothesis about the pattern of optic atrophy development in WS. This hypothesis must be confirmed only by a solid longitudinal prospective study of natural history, which may take time, or in vitro disease modeling, such as induced pluripotent stem cell–derived eye–brain organoids.

In conclusion, screening for *WFS1* mutations is mandatory in any patient with childhood onset optic atrophy. Our results support an early and progressive RGC axonal damage in patients with WS, which possibly precedes the RGC body degeneration with a distinct pattern from a classical mitochondrial optic neuropathy such as DOA. These findings shed light on the pathophysiology of the disease, impacting on prognosis, and may be relevant for the therapeutic window of opportunity and the clinical design of upcoming trials.

Acknowledgements: All authors have completed and submitted the ICMJE form for disclosure of potential conflicts of interest. Funding/Support: Supported by the Italian Ministry of Health (grant GR-2016-02361449 to L.C. and "Ricerca Corrente" funding to V.C. and V.P.). Financial Disclosures: P.B. reports consultancies for GenSight Biologics, has received speaker honoraria from Santhera Pharmaceuticals, Chiesi Farmaceutici, and Omikron Italia, and is the sub-investigator (SI) for clinical trials sponsored by GenSight Biologics and Santhera. None of these activities are related to conduction of this study and the writing of the manuscript. G.A. is a subinvestigator for clinical trials sponsored by GenSight Biologics and Santhera Pharmaceuticals. M.L.C. has received speaker honoraria from Chiesi Farmaceutici. M.R. reports consultancies from GenSight Biologics, honoraria from Santhera Pharmaceuticals, and is a Study Coordinator for clinical trials from GenSight Biologics and Santhera Pharmaceuticals. None of these activities are related to conduction of this study and the writing of the manuscript. L.C. has received speaker honoraria from First Class srl and University of Parma. R.B. has been a consultant for and on advisory boards for Medtronic, Roche, Theras, Novonordisk, Aventis, Abbott, Lilly, and Ypsomed and has received speaker honoraria from Lilly and Novonordisk. None of these activities are related to conduction of this study and the writing of the manuscript. M.C. has received consulting fees from GenSight Biologics and Santhera Pharmaceuticals and is the SI for clinical trials sponsored GenSight Biologics and Santhera Pharmaceuticals. None of these activities are related to this study. V.P. received speaker honoraria from Omikron Italia not related to the conduction of this study and the writing of the manuscript. F.B. is a consultant for Allergan, Bayer, Boehringer-Ingelheim, Fidia Sooft, Hofmann La Roche, Novartis, NTC Pharma, Sifi, Thrombogenics, and Zeiss. None of these activities are related to conduction of this study and the writing of the manuscript. V.C. reports consultant and advisory board activities with GenSight Biologics, Pretzel Therapeutics, Stealth Biotherapeutics and Chiesi Farmaceutici and honoraria from Chiesi Farmaceutici, First Class, and Medscape. None of these activities are related to conduction of this study and the writing of the manuscript. C.L.M. is a consultant for Chiesi Farmaceutici, Regulatory Pharma Net, and Thenewway srl, has received speaker honoraria from Santhera Pharmaceuticals, Chiesi Farmaceutici, Regulatory Pharma Net, Thenewway srl, First Class srl, and Biologix, and has acted as the PI/SI for clinical trials sponsored GenSight Biologics and Santhera Pharmaceuticals. None of these activities are related to conduction of this study and the writing of the manuscript. The other authors declare no financial disclosures. All authors attest that they meet the current ICMJE criteria for authorship.

REFERENCES

1. Barrett TG, Bundey SE, Macleod AF. Neurodegeneration and diabetes: UK nationwide study of Wolfram (DIDMOAD) syndrome. *Lancet*. 1995;346(8988):1458–1463.
2. Inoue H, Tanizawa Y, Wasson J, et al. A gene encoding a transmembrane protein is mutated in patients with diabetes mellitus and optic atrophy (Wolfram syndrome). *Nat Genet*. 1998;20(2):143–148.
3. de Heredia ML, Cleries R, Nunes V. Genotypic classification of patients with Wolfram syndrome: insights into the natural history of the disease and correlation with phenotype. *Genet Med*. 2013;15(7):497–506.
4. Chaussenot A, Bannwarth S, Rouzier C, et al. Neurologic features and genotype-phenotype correlation in Wolfram syndrome. *Ann Neurol*. 2011;69(3):501–508.
5. Li LP, Venkataraman L, Chen S, Fu HJ. Function of WFS1 and WFS2 in the central nervous system: implications for Wolfram syndrome and Alzheimer's disease. *Neurosci Biobehav Rev*. 2020;118:775–783.
6. Paillusson S, Stoica R, Gomez-Suaga P, et al. There's something wrong with my MAM; the ER-mitochondria axis and neurodegenerative diseases. *Trends Neurosci*. 2016;39(3):146–157.
7. Loncke J, Kaasik A, Bezprozvanny I, et al. Balancing ER-mitochondrial Ca2+fluxes in health and disease. *Trends Cell Biol*. 2021;31(7):598–612.
8. Angebault C, Fauconnier J, Patergnani S, et al. ER-mitochondria cross-talk is regulated by the Ca2+ sensor NCS1 and is impaired in Wolfram syndrome. *Sci Signal*. 2018;11(553):eaaq1380.
9. La Morgia C, Maresca A, Amore G, et al. Calcium mishandling in absence of primary mitochondrial dysfunction drives cellular pathology in Wolfram syndrome. *Sci Rep*. 2020;10(1):4785.
10. Maresca A, Carelli V. Molecular mechanisms behind inherited neurodegeneration of the optic nerve. *Biomolecules*. 2021;11(4):496.
11. Bu XD, Rotter JI. Wolfram-syndrome - a mitochondrial-mediated disorder. *Lancet*. 1993;342(8871):598–600.
12. Barrett TG, Scott-Brown M, Seller A, et al. The mitochondrial genome in Wolfram syndrome. *J Med Genet*. 2000;37(6):463–466.

13. Delprat B, Maurice T, Delettre C. Wolfram syndrome: MAMs' connection? *Cell Death Dis*. 2018;9(3):364.
14. Grenier J, Meunier I, Daien V, et al. WFS1 in optic neuropathies: mutation findings in nonsyndromic optic atrophy and assessment of clinical severity. *Ophthalmology*. 2016;123(9):1989–1998.
15. Hershey T, Lugar HM, Shimony JS, et al. Early brain vulnerability in Wolfram syndrome. *Plos One*. 2012;7(7):e40604.
16. Rando TA, Horton JC, Layzer RB. Wolfram syndrome - evidence of a diffuse neurodegenerative disease by magnetic-resonance-imaging. *Neurology*. 1992;42(6):1220–1224.
17. Lugar HM, Koller JM, Rutlin J, et al. Evidence for altered neurodevelopment and neurodegeneration in Wolfram syndrome using longitudinal morphometry. *Sci Rep*. 2019;9(1):6010.
18. Samara A, Lugar HM, Hershey T, Shimony JS. Longitudinal assessment of neuroradiologic features in Wolfram syndrome. *AJNR Am J Neuroradiol*. 2020;41(12):2364–2369.
19. Pakdemirli E, Karabulut N, Bir LS, Sermez Y. Cranial magnetic resonance imaging of Wolfram (DIDMOAD) syndrome. *Australas Radiol*. 2005;49(2):189–191.
20. Ito S, Sakakibara R, Hattori T. Wolfram syndrome presenting marked brain MR imaging abnormalities with few neurologic abnormalities. *AJNR Am J Neuroradiol*. 2007;28(2):305–306.
21. Samara A, Rahn R, Neyman O, et al. Developmental hypomyelination in Wolfram syndrome: new insights from neuroimaging and gene expression analyses. *Orphanet J Rare Dis*. 2019;14(1):279.
22. Hoekel J, Chisholm SA, Al-Lozi A, et al. Ophthalmologic correlates of disease severity in children and adolescents with Wolfram syndrome. *J AAPOS*. 2014;18(5):461–465 e1.
23. Zmyslowska A, Fendler W, Niwald A, et al. Retinal thinning as a marker of disease progression in patients with Wolfram syndrome. *Diabetes Care*. 2015;38(3):e36–e37.
24. Zmyslowska A, Fendler W, Waszczykowska A, et al. Retinal thickness as a marker of disease progression in longitudinal observation of patients with Wolfram syndrome. *Acta Diabetol*. 2017;54(11):1019–1024.
25. Zmyslowska A, Waszczykowska A, Baranska D, et al. Optical coherence tomography and magnetic resonance imaging visual pathway evaluation in Wolfram syndrome. *Dev Med Child Neurol*. 2019;61(3):359–365.
26. Yamamoto H, Hofmann S, Hamasaki DI, et al. Wolfram syndrome 1 (WFS1) protein expression in retinal ganglion cells and optic nerve glia of the cynomolgus monkey. *Exp Eye Res*. 2006;83(5):1303–1306.
27. Schmidt-Kastner R, Kreczmanski P, Preising M, et al. Expression of the diabetes risk gene wolframin (WFS1) in the human retina. *Exp Eye Res*. 2009;89(4):568–574.
28. Shannon P, Becker L, Deck J. Evidence of widespread axonal pathology in Wolfram syndrome. *Acta Neuropathol*. 1999;98(3):304–308.
29. Ross-Cisneros FN, Pan BX, Silva RA, et al. Optic nerve histopathology in a case of Wolfram syndrome: a mitochondrial pattern of axonal loss. *Mitochondrion*. 2013;13(6):841–845.
30. Mota A, Fonseca S, Ferreira CS, Faria O, Silva SE. Retinal nerve fiber layer thickness analysis with optical coherence tomography in Wolfram Syndrome. *Int J Ophthalmic Pathol*. 2013;2(1):1–4.
31. Schmitz B, Schaefer T, Krick CM, et al. Configuration of the optic chiasm in humans with albinism as revealed by magnetic resonance imaging. *Invest Ophthalmol Vis Sci*. 2003;44(1):16–21.
32. Ather S, Proudlock FA, Welton T, et al. Aberrant visual pathway development in albinism: from retina to cortex. *Hum Brain Mapp*. 2019;40(3):777–788.
33. Maresky HS, Ben Ely A, Bartischovsky T, et al. MRI measurements of the normal pediatric optic nerve pathway. *J Clin Neurosci*. 2018;48:209–213.
34. Colosimo A, Guida V, Rigoli L, et al. Molecular detection of novel WFS1 mutations in patients with Wolfram syndrome by a DHPLC-based assay. *Hum Mutat*. 2003;21(6):622–629.
35. Barboni P, Savini G, Parisi V, et al. Retinal nerve fiber layer thickness in dominant optic atrophy measurements by optical coherence tomography and correlation with age. *Ophthalmology*. 2011;118(10):2076–2080.
36. Sakakibara Y, Sekiya M, Fujisaki N, et al. Knockdown of wfs1, a fly homolog of Wolfram syndrome 1, in the nervous system increases susceptibility to age- and stress-induced neuronal dysfunction and degeneration in Drosophila. *PLoS Genet*. 2018;14(1):e1007196.
37. Sharma S, Chitranshi N, Wall RV, et al. Trans-synaptic degeneration in the visual pathway: neural connectivity, pathophysiology, and clinical implications in neurodegenerative disorders. *Surv Ophthalmol*. 2022;67(2):411–426.
38. Labauge P, Renard D, Chaussenot A. Paquis-Flucklinger V. Neurological picture. Wolfram syndrome associated with leukoencephalopathy. *J Neurol Neurosurg Psychiatry*. 2010;81(8):928.
39. Bueno GE, Ruiz-Castaneda D, Martinez JR, et al. Natural history and clinical characteristics of 50 patients with Wolfram syndrome. *Endocrine*. 2018;61(3):440–446.